Metabolic Rescue of Obese Adipose-Derived Stem Cells by Lin28/*Let7* Pathway

Laura M. Pérez,[1] Aurora Bernal,[1] Nuria San Martín,[1] Margarita Lorenzo,[2†]
Sonia Fernández-Veledo,[3,4] and Beatriz G. Gálvez[1]

Adipose-derived stem cells (ASCs) are promising candidates for autologous cell-based regeneration therapies by virtue of their multilineage differentiation potential and immunogenicity; however, relatively little is known about their role in adipose tissue physiology and dysfunction. Here we evaluated whether ASCs isolated from nonobese and obese tissue differed in their metabolic characteristics and differentiation potential. During differentiation to mature adipocytes, mouse and human ASCs derived from nonobese tissues both increased their insulin sensitivity and inhibition of lipolysis, whereas obese-derived ASCs were insulin-resistant, showing impaired insulin-stimulated glucose uptake and resistance to the antilipolytic effect of insulin. Furthermore, obese-derived ASCs showed enhanced release of proinflammatory cytokines and impaired production of adiponectin. Interestingly, the delivery of cytosol from control ASCs into obese-derived ASCs using a lipid-based, protein-capture methodology restored insulin sensitivity on glucose and lipid metabolism and reversed the proinflammatory cytokine profile, in part due to the restoration of Lin28 protein levels. In conclusion, glucose and lipid metabolism as well as maturation of ASCs is truncated in an obese environment. The reversal of the altered pathways in obese cells by delivery of normal subcellular fractions offers a potential new tool for cell therapy. *Diabetes* 62:2368–2379, 2013

Adipose tissue is now recognized as an important endocrine and metabolic organ that, when accumulated in excess, increases the risk of chronic diseases such as diabetes, stroke, and arterial hypertension (1). Recently, new mechanisms that control the obesity phenotype have been identified such as the equilibrium between white and brown adipose tissue, the localization of adipose mass (visceral vs. ventral), and the presence of adipose stem cells (ASCs) and mesenchymal stem cells (MSCs) (1–4). Although the relative importance of fat tissue type and localization are being actively unraveled, the role of stem cells in adipose tissue physiology and dysfunction is still poorly understood.

Adult stem cells are multipotent cells that contribute to the homeostasis of various organs, including adipose tissue. ASCs are a class of MSCs localized in adipose tissue that have attracted increasing interest because of their potential to differentiate into adipogenic, osteogenic, chondrogenic, and other mesenchymal lineages (5–8). Other clinically attractive properties attributed to ASCs include proangiogenic and anti-inflammatory actions (9–11). Moreover, depending on the environmental conditions, ASCs can be beneficial or detrimental to health. ASCs thus represent a possible target for therapies aimed at modulating the response of the body to obesity and diabetes as well as a potential tool for regenerative medicine.

Adipocytes are central to the control of energy balance and lipid homeostasis (12). In response to prolonged obesity, adipocytes become hypertrophic, and new adipocytes are required to counter the metabolic dysfunction of the hypertrophic cells (13,14). It has been postulated that the adipose tissue depots of obese individuals have already committed all of their stem cell reserves to the adipocyte lineage and, therefore, have no capacity to generate new adipocytes (15–17).

In this study, we demonstrate that the differentiation of mouse and human adipose MSCs into mature well-functioning adipocytes is truncated in an obese environment, resulting in impaired metabolic function. We also validate a novel approach to restore normal adipocyte metabolic responsiveness in obese-derived stem cells by cytosolic transfer.

RESEARCH DESIGN AND METHODS

Reagents. Culture media and anti-*Let7* microRNA inhibitor were purchased from Invitrogen (Paisley, U.K.). 2-deoxy-D[1-3H]glucose (11.0 Ci/mmol) was from GE Healthcare (Rainham, U.K.). Antibodies to GLUT4, insulin receptor substrate 1 (IRS1), and phospho-IRS1 (Tyr612) and anticaveolin-1, anti–β-tubulin, and anti–Pi3-kinase were purchased from Millipore (Bedford, MA). An antibody to tumor necrosis factor-α (TNF-α) and recombinant TNF-α cytokine were purchased from BD Pharmingen (Franklin Lakes, NJ). An antibody to monocyte chemoattractant protein-1 (MCP-1) was purchased from R&D Systems (Minneapolis, MN), and recombinant MCP-1 cytokine was from Reprokine (Valley Cottage, NJ). An antibody to Lin28b was purchased from Abcam (Cambridge, U.K.), and purified full-length Lin28b protein was obtained from Applied Biological Materials Inc. (Richmond, BC, Canada). The mirCury LNA microRNA *Let7* inhibitor was purchased from Exiqon (Vedbaek, Denmark). Unless otherwise stated, all other reagents were purchased from Sigma-Aldrich (Poole, Dorset, U.K.).

Animals. C57BL/6 mice and leptin-deficient *ob/ob* mice (18) were obtained from Charles River (Wilmington, MA) and maintained and used in accordance with the National Institutes of Health Animal Care and Use Committee.

Mice were killed by cervical dislocation for sample collection. DIO rodent purified high-fat diet (formula 58Y1) was obtained from TestDiet (IPS Product Supplies Ltd., London, U.K.).

Isolation of mouse and human ASCs. ASCs were isolated by the explant method (19). Briefly, small pieces of subcutaneous adipose tissue were collected from five control and five obese mice (4 months old) and placed on gelatin-coated plates (Fig. 1A). After 7 days, rounded cells emerging from the explants were selected, cloned by limiting dilution, and grown to obtain ASCs.
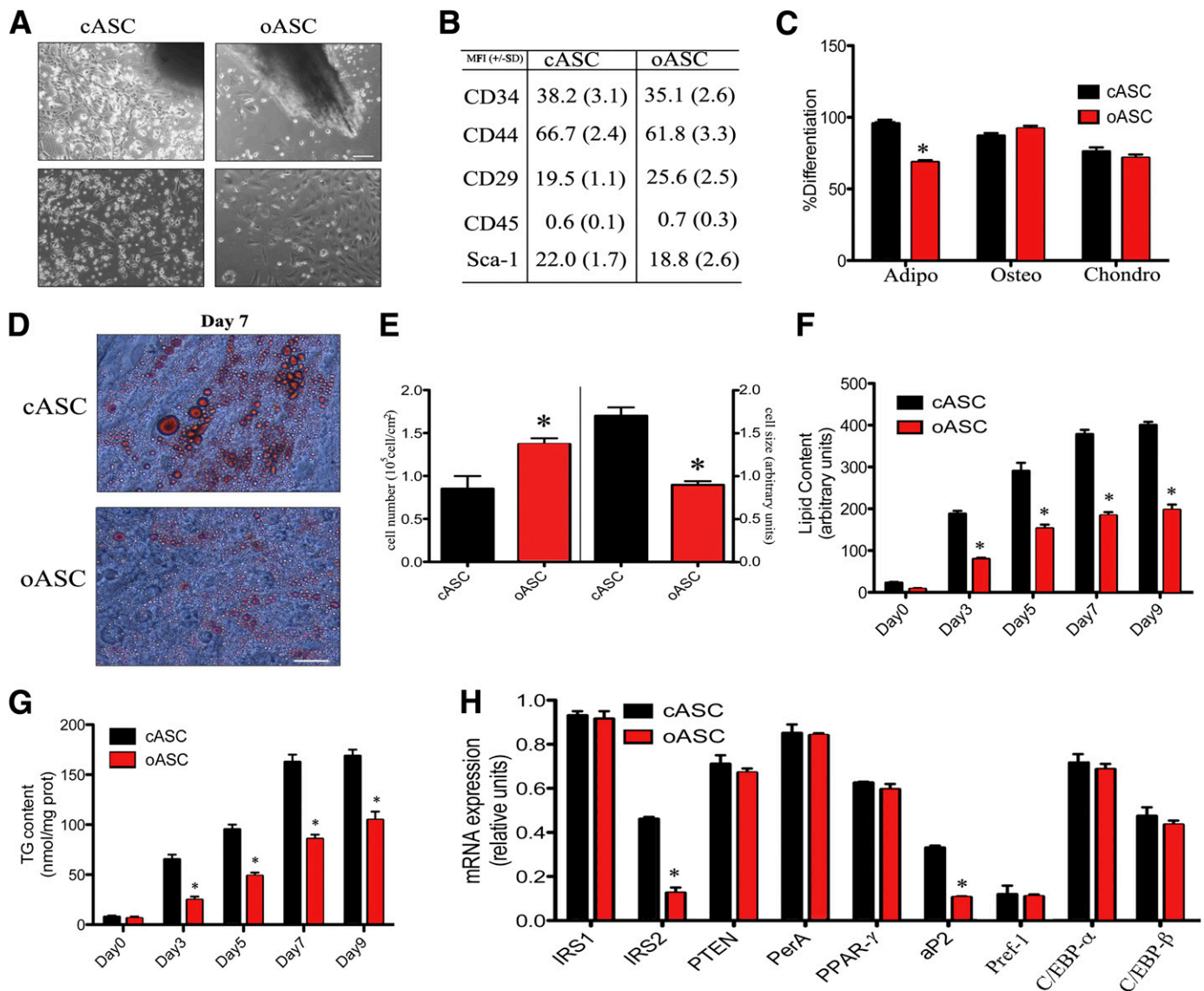
FIG. 1. Isolation and differentiation of ASCs. *A*: Proliferating ASCs emerging from adipose tissue explants. Bar, 150 μm. *B*: Flow cytometry characterization of ASCs from control (C57BL/6) and obese (*ob/ob*) mice. Mean fluorescence intensity (MFI) plus standard deviations of five independent experiments are shown. *C*: Percentages of differentiation into adipose (Adipo) (Oil Red O staining), chondrogenic (Chondro) (To-luidine Blue staining), or osteogenic (Osteo) (Alizarin Red staining) tissues of five different cASCs and oASCs were quantified by histochemistry. *P < 0.04. *D*: Representative image of Oil Red O staining in cASCs and oASCs differentiated for 7 days into adipocytes. Bar, 30 μm. *E*: Cell number (*left*) and cell size (*right*) analyzed by flow cytometry in cASCs and oASCs at day 7 of differentiation (*n* = 5). *F*: Intracellular lipid accumulation in differentiating ASCs (*n* = 5). *P < 0.03. *G*: Triglyceride (TG) content in differentiating cASCs and oASCs (*n* = 5). *P < 0.04. *H*: Gene expression profile of cASCs and oASCs at day 7 of differentiation (*n* = 5). *P < 0.02.

Independent ASC clonal lines obtained from five different mice were first characterized by morphology (Fig. 1*A*) and by flow cytometry for the surface antigens that have been used to specifically define this population (3), namely Sca-1^{+}, CD34^{+}, CD44^{+}, CD29^{+}, and CD45^{−} (Fig. 1*B*). The cells for these clones were derived from control (c) or obese (o) and named cASCs or oASCs, respectively. We obtained 2 clones from each of the 5 obese mice, obtaining a total of 10 oASCs clones; with control explants, we obtained 10 independent clones from each of 5 animals. Finally, five oASC and five cASC clones derived from independent animals were selected randomly, and because all expressed similar surface markers and presented similar morphology, were pooled respectively as a population of oASC or cASC and used for experiments. ASCs were maintained on gelatin-coated plates in Dulbecco's modified Eagle's medium (DMEM) containing 10% FBS and supplemented with glutamine and penicillin/streptomycin.

Human adipose samples were obtained from patients after bariatric surgery. Informed consent was obtained from all subjects, and the sample collection conformed to the principles set out in the World Medical Association Declaration of Helsinki and the National Institutes of Health Belmont Report. ASCs were isolated from five control patients (BMI <22 kg/m²) and five obese patients (BMI >30 kg/m²) by the explant method, similar to the protocol used above for mice (19,20). Human ASCs were also characterized by surface marker expression and named as hASCs. Human primary ASCs were also purchased from Lonza (Walkersville, MD); one derived from an obese patient (BMI 31 kg/m²) (PT5006 lot 4308 stock 32) and the other from a nonobese patient (BMI <22 kg/m²) (PT4504 lot 4028 stock 27). All cells were maintained in the medium supplied with the PT4505-ADSC Bullekit (Lonza).

Cell culture and treatments. To induce adipogenic differentiation, ASCs were cultured in serum-free DMEM/F12 medium (1:1) supplemented with 10 μg/mL transferrin, 15 mmol/L NaHCO₃, 15 mmol/L HEPES, 33 μmol/L biotin, 17 μmol/L pantothenate, 1 nmol/L insulin, 20 pmol/L triiodothyronine, and 1 μmol/L cortisol, plus antibiotics. Accumulation of triglycerides in adipocytes was visualized by staining formalin-fixed cells with Oil Red O. Triglyceride accumulation was assessed microscopically, and Oil Red O concentration was quantified spectrophotometrically at 510 nm. Lipid content was also analyzed enzymatically with a triglyceride determination kit. To measure the osteogenic potential of the ASCs, 2 × 10⁴ cells were incubated in DMEM containing 10% FBS and supplemented with glutamine and penicillin/streptomycin until a confluent layer was achieved. Then, osteogenic medium was added, containing

Iscove's modified Dulbecco's medium supplemented with 9% FBS, 9% heparan sulfate, 2 mmol/L L-glutamine, 100 units/mL penicillin, 100 μg/mL streptomycin, 50 ng/mL L-thyroxine, 20 mmol/L β-glycerol phosphate, 100 nmol/L dexamethasone, and 50 μmol/L ascorbic acid. Medium was refreshed every 3 to 4 days. After 17 days of culture cells were fixed in 10% formalin and stained with 10% Alizarin Red, and osteocytes were quantified under a microscope. To measure the chondrogenic differentiation of ASCs, 5×10^5 cells were incubated in 500 μL complete chondrogenic medium, containing Iscove's modified Dulbecco's medium, 100 nmol/L dexamethasone, 50 μg/mL ascorbic acid, 40 μg/mL L-proline, 1 mmol/L sodium pyruvate, 100 units/mL penicillin, 100 μg/mL streptomycin, 10 ng/mL transforming growth factor-β3, and 100 ng/mL bone morphogenetic protein 2. The medium was changed three times a week. After 21 days, cells were stained with Toluidine Blue sodium borate, and chondrocytes were quantified under a microscope. Metabolic and signaling studies were performed in adipocytes and ASCs previously cultured overnight in serum-free medium containing low glucose (5.5 mmol/L).

Gene expression profiling. Total RNA from different organs was isolated with TRIzol (Invitrogen, Carlsbad, CA) and reverse transcribed using Platinum Taq DNA polymerase (Invitrogen). Real-time quantitative PCR was performed on an Mx3000P real-time PCR system (Stratagene, La Jolla, CA). Each cDNA sample was amplified in duplicate using SYBR Green Supermix chemistry (BioRad, Hercules, CA). The following murine primers were used in this study: *IRS1* (forward [Fw], CTTCTGTCAGGTGTCCATCC; reverse [Rv], CTCTGCAGCAATGCCTGTTC), *IRS-2* (Fw, ACAATGGTGACTACACCGAG; Rv, CTGCTTTTCCTGAGAGAGAC), *PTEN* (Fw, AATTCCCAGTCAGAGGCGCTATGT; Rv, GATTGCAAGTTCCGCCACTGAACA), *PerA* (Fw, GGCCTGGACGACAAAACC; Rv, CAGGATGGGCTCCATGAC), *PPAR-γ* (Fw, ATTGACCCAGAAAGCGATTC; Rv, CAAAGGAGTGGGAGTGGTCT), *aP2* (Fw, AACCTTAGATGGGGGTGTCCTG; Rv, TCGTGGAAGTGACGCCTTTC), *Pref-1* (Fw, AGCTGGCGGTCAATATCATC; Rv, AGCTCTAAGGAACCCCCGGTA), *C/EBP-α* (Fw, TTACAACAGGCCAGGTTTCC; Rv, CTCTGGGATGGATCGATTGT), *C/EBP-β* (Fw, ACCGGGTTTCGGGACTTGA; Rv, GTTGCGTAGTCCCGTGTCCA), and *LIN28b* (Fw, GACCCAAAGGGAAGACACTA; Rv, TCTTCCCTGAGAACTCGCGG).

For measurement of *Let7* expression, RNA (10 ng) from ASCs or mASCs was obtained and used in the PCR. MirCury locked nucleic acid (LNA)–specific PCR mouse and human primers were purchased from Exiqon (Vedbaek, Denmark).

Immunoblot analysis. Cellular proteins were separated by SDS-PAGE, transferred to Immobilon membranes, and blocked using standard techniques (21). After antibody incubation, immunoreactive bands were visualized using the enhanced chemiluminescence (ECL-Plus) method (GE Healthcare).

Glucose transport and GLUT4 translocation assays. Glucose uptake was measured during the last 10 min of culture by incorporation of labeled 2-deoxyglucose into cells and expressed as the percentage of stimulation over basal, as previously described (22). Plasma membrane and internal membrane subcellular fractions, together with whole lysates from differentiated ASCs, were prepared (22) and immunoblotted with GLUT4, caveolin-1, phosphatidylinositide 3-kinases (PI3K), or tubulin antibodies.

Determination of lipolytic rate. Lipolysis (triglyceride breakdown) was estimated by the release rate of glycerol and nonesterified fatty acids (NEFA) from cells. Adipocytes were cultured overnight in serum-free medium before assay. After washing, cells were incubated at 37°C for 3 h as described in Fig. 2C and D, and glycerol release was measured enzymatically with a free-glycerol determination kit. At the same time, NEFA release was determined by an enzymatic colorimetric test (Wako Chemicals, Neuss, Germany). Results are expressed as nanomoles of glycerol per NEFA per milligram of protein per 3 h.

Preparation of adipocyte-conditioned media and measurement of adipokine release. ASCs were cultured overnight in serum-free medium, and the medium was retained as adipocyte-conditioned media. Adipokines were measured using Luminex xMAP technology with multiplex immunoassays (LincoPlex) for simultaneous quantitative determination of adiponectin, MCP-1 and TNF-α (Millipore), with detection limits of 75.2, 0.6, and 0.09 pg/mL, respectively.

Cytosolic fraction isolation and delivery. Cytosolic fractions (CFs; 100 μL) were obtained from 1×10^6 cASCs, oASCs, and control fibroblasts using the Complete Cell Fractionation Kit (BioVision, Milpitas, CA). After corroborating purity by Western blot and agarose gel electrophoresis, 25 μL functional CFs (one-fourth of the total volume obtained) were delivered to 250,000 cells of oASCs or cASCs seeded on a six-well plate, using the lipid-based protein-capture reagent Pro-DeliverIN (OZ Biosciences, Marseille, France). Eight independent transfer experiments were performed on a pooled-population of five lean clones and another eight independent transfer experiments on a pooled-population of five obese clones ($n = 8$). The cytosol-modified ASCs (mASCs) were analyzed in the assays described above. Inactivated fractions were prepared by treatment with 100 μg/mL proteinase-K, or with 10 μg/mL

RNAase/DNAase cocktail (Ambion, Life Technologies). Before delivery, proteinase-K was inactivated by adding a specific inhibitor (25 nmol/L diisopropyl phosphorofluoridate), and RNAase/DNAase cocktail was inactivated by adding 5 mmol/L EGTA. Controls for the processing were performed in parallel to avoid unspecific effects (data not shown).

Metabolic labeling. cASC, oASC, or mASC were plated onto 24-well plates and incubated in 1 mL DME (free methionine medium) overnight. 3λ of Met ^{35}S (New England BioLabs, Ontario, Canada) were added to the cultures and incubated for 5 h at 37°C. Supernatant was removed and cultures were treated with 1 mL PBS/0.05% Tween, mixed, and centrifuged for 30 s at 6000 rpm. Nondenaturing loading buffer was added, and samples were boiled at 5 min and ran in a SDS-PAGE gel. After incubation with 30% ethyl alcohol/10% acetic acid, membranes were exposed to a phosphoimager screen. A similar protocol was used for the immunoprecipitation, but before the loading buffer was added, samples were incubated for 1 h with anti-Lin28 antibody and normal immunoprecipitation was performed. In some cases, cASC- and oASC-labeled cells were processed for isolation of CFs before the immunoprecipitation was performed.

Statistical analysis. All data are represented as mean ± SEM from 5 to 10 independent experiments (n = number of independent repeated experiments). Comparisons between two groups were by Student t test. One-way or two-way ANOVA were used as required by the assay. Differences between groups were considered statistically significant at $P < 0.05$.

RESULTS

Isolation and characterization of ASCs from mouse explants.

To examine the properties of adipose tissue–derived MSCs originating from normal and obese environments, we collected adipose tissue explants from the subcutaneous adipose mass of wild-type (WT) C57 mice and leptin-deficient *ob/ob* mutant mice. MSCs were isolated using the explant technique (23), and termed cASCs and oASCs depending on their origin from WT (c) or obese (o) mice (Fig. 1A). Flow cytometry analysis confirmed that both types of ASCs were positive for CD44, Sca-1, CD34, and CD29, and negative for CD45, independently of the mouse or clone used (Fig. 1B). Furthermore, all ASCs were capable of differentiation to the three mesenchymal lineages (adipogenic, osteogenic, and chondrogenic) in defined medium (Fig. 1C). Together, these data identify an ASC subpopulation from both normal and obese animals (3). Interestingly, although oASCs were capable of forming mature adipocytes, as defined by Oil Red O staining of lipid droplets, the percentage of adipocytes was significantly lower compared with cASCs (Fig. 1C). Analysis of Oil Red O staining after 7 days of differentiation revealed that cASCs rapidly differentiated into well-defined mature adipocytes (Fig. 1D). In contrast, oASCs did not reach complete maturity, and the derived adipocytes exhibited a smaller cell size, with smaller lipid droplets together with a hyperplasic phenotype (Fig. 1D and E). Moreover, biochemical analysis of differentiated oASCs revealed a 50% reduction in the quantity of lipids (Fig. 1F), and triglycerides (Fig. 1G), compared with cASCs over the same period.

To corroborate the differences in maturity between the two populations, we next analyzed the expression of a subset of established adipogenic markers. No changes were observed in *IRS1*, phosphatase and tensin homolog (*PTEN*), perilipin (*PerA*), preadipoctye factor 1 (*Pref-1*), CCAAT/enhancer binding protein α and β (*C/EBP-α* and *C/EBP-β*), and peroxisome proliferator-activated receptor γ (*PPAR-γ*) expression, whereas a reduction in expression of insulin receptor substrate 2 (IRS2) and adipocyte fatty acid binding protein (aP2) was observed in oASCs compared with cASC (Fig. 1H). Experiments performed with ASCs isolated from mice fed a high-fat diet for 12 weeks (hfASCs) produced similar results to those derived from

ob/ob mice (Supplementary Fig. 1*A*–*D*), including differentiation capability, triglyceride content, and gene expression pattern. Taken together, these results show that ASCs derived from an obese environment have an impaired ability to differentiate correctly compared with ASCs derived from a nonobese environment.

Metabolic properties of ASCs. Having shown that differentiation of oASCs led to a partially immature phenotype, we next wanted to ascertain physiological functionality. Given that a primary role of adipocyte tissue is to act as an energy reservoir, we monitored the ability of ASCs to take up glucose in response to insulin signaling. Unsurprisingly, insulin (10 nmol/L)–stimulated glucose uptake in cASCs produced a maximal stimulation of approximately threefold after 7 days of differentiation (Fig. 2*A*, *left panel*). In contrast, basal glucose uptake in 7-day differentiated oASCs was fivefold higher than in corresponding cultures of differentiated cASCs, and incubation with insulin produced no additional effect, indicating that these cells were nonresponsive to insulin (Fig. 2*A*, *right panel*). We hypothesized that the basal glucose uptake in oASCs is upregulated to such an extent that the cells become unresponsive to further stimulation. This upregulation could be due to a higher glucose transport on oASC, and therefore, we proceeded to analyze the expression and translocation of the GLUT4 transporter. Interestingly, GLUT4 was highly expressed in whole lysates in oASC compared with cASC (Fig. 2*B*, *right panels*). Furthermore, insulin was shown to

stimulate GLUT4 translocation to the plasma membrane in cASC-derived adipocytes differentiated for 7 days, whereas this effect was impaired in oASC-derived adipocytes (Fig. 2*B*).

Continuing this assessment, we next measured lipid metabolism by monitoring the release of glycerol and NEFA as an index of lipolysis. Stimulation of lipolysis by the β-adrenergic agonist isoproterenol resulted in a fivefold increase of glycerol release in 7-day differentiated cASC-derived adipocytes, which could be blunted significantly by preincubation with insulin (Fig. 2*C*). In contrast, oASC-derived adipocytes, although exhibiting a higher basal rate of glycerol release, were less responsive to agonist stimulation by isoproterenol, and again, were resistant to the inhibiting effects of insulin (Fig. 2*C*). A similar pattern was observed by measurement of fatty acid release (Fig. 2*D*). Interestingly, the basal lipolysis rate of oASCs was elevated compared with levels in cASCs, possibly due to a significant decrease in the expression of aP2 in these cells (Fig. 1*H*) or to a dysregulated functionality of perilipins in oASCs. At the molecular level, examination of insulin-stimulated tyrosine phosphorylation on IRS1 showed that the maximal activation at 7 days in cASC-derived adipocytes was significantly reduced in oASC-derived adipocytes (Fig. 2*E*). Collectively, these results suggest that oASCs show resistance to the antilipolytic effect of insulin and also have a reduced response to isoproterenol stimulation.
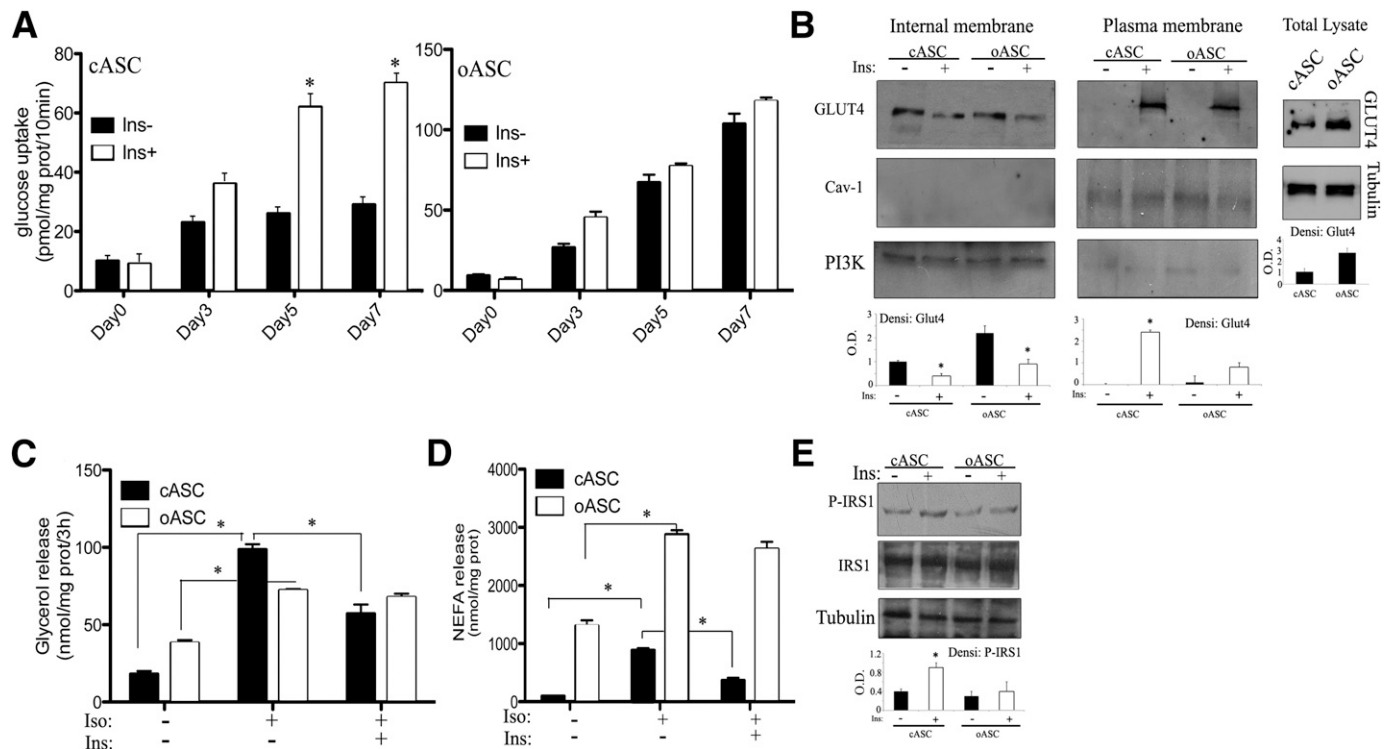
FIG. 2. Glucose and lipid metabolism during ASC differentiation. *A*: Insulin-stimulated glucose uptake by cASC and oASC cultures at different stages of differentiation. Cells were stimulated with 10 nmol/L insulin (Ins) for 30 min. Results are expressed as pmol/mg protein (prot) per 10 min (*n* = 6), *P < 0.01. *B*: GLUT4 expression in 7-day differentiated cASCs and oASCs. Cells were stimulated for 20 min with 10 nmol/L insulin and lysed or fractioned. Plasma and internal membrane proteins, together with whole lysates, were analyzed by Western blot with anti–GLUT4 antibody; anti-caveolin (Cav)1, anti-PI3K, or anti-tubulin antibodies were used as controls. Densitometric bar graph quantification of three independent membranes is shown. O.D., optical density. *P < 0.05. *C*: Glycerol release from 7-day differentiated cASCs and oASCs. Cells were treated with 10 nmol/L insulin for 1 h before stimulation with 1 μmol/L isoproterenol (Iso) for 15 min (*n* = 6). *P < 0.03. *D*: NEFA release in 7-day differentiated ASCs treated as in *C* (*n* = 5). *P < 0.05. *E*: Activation of IRS1: 7-day differentiated ASCs were stimulated with 10 nmol/L insulin for 10 min and lysed. Total protein was analyzed by Western blot with anti-phospho- and anti-total IRS1, together with antitubulin antibodies. Densitometric bar graph quantification of three independent membranes is shown. *P < 0.05.

cASCs and oASCs have distinct secretion profiles. It is now recognized that adipocytes, as well as functioning as storage cells, can also secrete a number of highly diverse factors, termed adipokines, including classical cytokines, growth factors, and hormones (24), which together increase the functionality of adipose tissue (25). Examination of adipokine secretion patterns during differentiation revealed that whereas adiponectin content in conditioned medium of cASC-derived adipocytes peaked between days 5 and 7, in oASC-derived adipocyte cultures, secreted adiponectin began to decline from day 5 (Fig. 3A). Interestingly, other adipokines showed disparate release patterns from cASC and oASC cells, with secretion of MCP-1 and TNF-α only slightly detectable in medium from cASC-derived adipocytes at any time point compared with a robust secretion in differentiated oASC-derived adipocyte cultures (Fig. 3B and C). To test whether factors secreted by cASC-derived adipocytes could modulate insulin
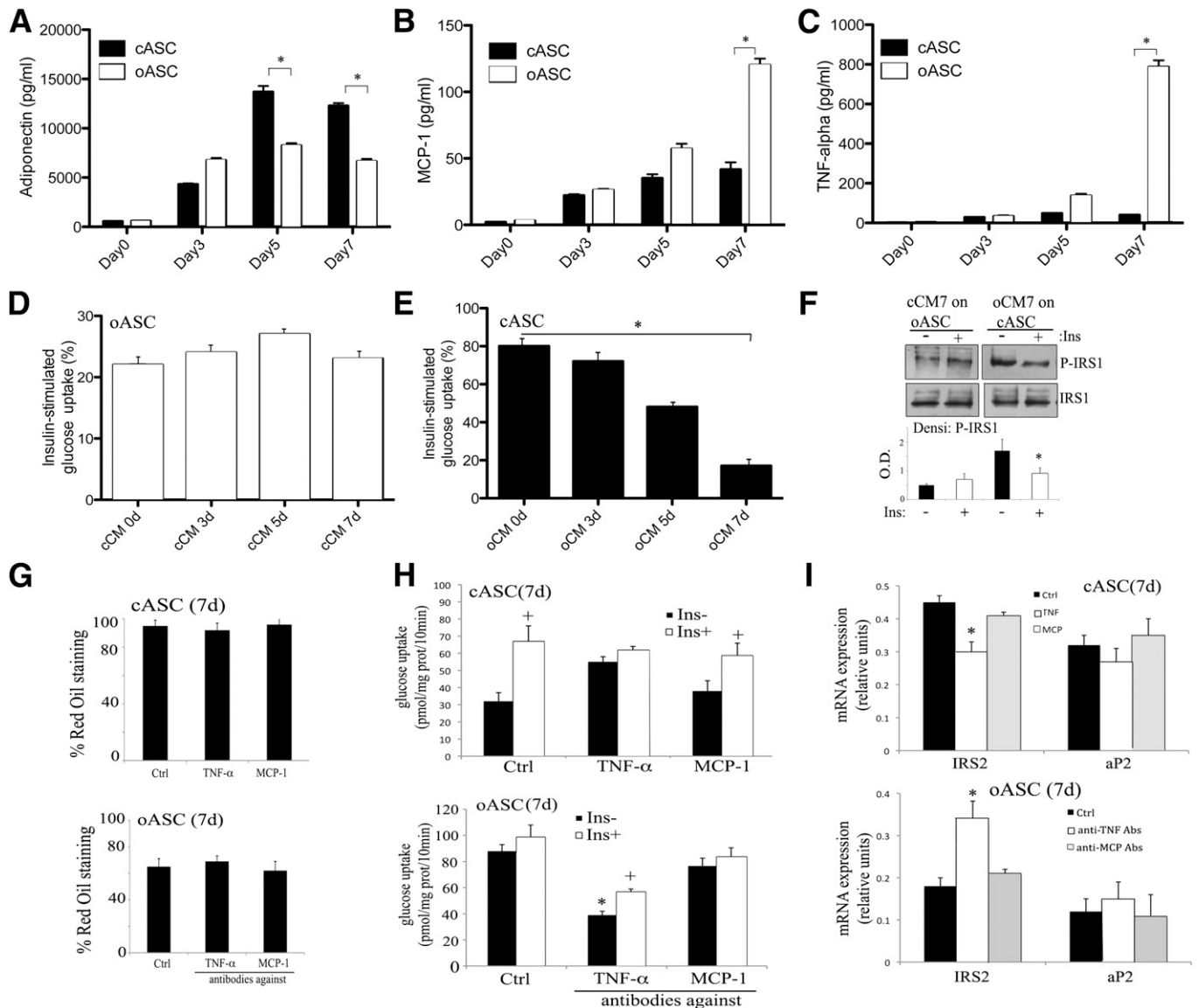
FIG. 3. The altered cytokine profile of oASCs transfers insulin resistance to cASC-derived adipocytes. A–C: cASCs and oASCs were differentiated for up to 7 days and cultured overnight in serum-free medium. Adiponectin, MPC-1, and TNF-α content were measured in conditioned medium (pg/mL) (n = 4). *P < 0.01. D and E: Effect of adipocyte-conditioned medium on insulin-stimulated glucose uptake. cASC- or oASC-derived 7-day adipocytes were cultured in the presence of conditioned medium from cCM or oCM for 24 h (n = 8). Cells were then maintained for 2 h in serum-free, low-glucose medium before stimulating with insulin (100 nmol/L, 30 min). Data are expressed as the percentage of the induced glucose uptake (stimulated – basal) in nontreated cells at 7-day differentiation (n = 8). *P < 0.01. F: oASC- and cASC-derived 7-day adipocytes were pretreated (24 h) with cCM or oCM of day 7, stimulated with 100 nmol/L Ins for 5 min, and lysates analyzed by Western blot with antibodies against phosphorylated and total IRS1. Densitometric bar graph quantification of three independent membranes is shown. O.D., optical density. *P < 0.05. G: Differentiation into mature adipocytes by cASC in the presence or absence of 1 ng/mL TNF-α or 0.2 ng/mL MCP-1 cytokines and by oASC in the presence or absence of 10 ng/mL anti–TNF-α or anti–MCP-1 antibodies. Oil Red O quantification of five independent experiments is shown. H: Insulin-stimulated glucose uptake by cASC-derived 7-day adipocytes in the presence or absence of 1 ng/mL TNF-α or 0.2 ng/mL MCP-1 cytokines and by oASC-derived 7-day adipocytes in the presence or absence of 10 ng/mL anti–TNF-α or anti–MCP-1 antibodies. Cells were stimulated with 10 nmol/L insulin (Ins) for 30 min. Results are expressed as pmol glucose/mg protein (prot)/10 min (n = 5). *P < 0.03, +P < 0.05. I: Gene expression profile at day 7 of differentiation of adipocytes derived from cASCs in the presence or absence of 1 ng/mL TNF-α or 0.2 ng/mL MCP-1 cytokines or from oASCs in the presence or absence of 10 ng/mL anti–TNF-α or anti–MCP-1 antibodies (Abs) (n = 5). *P < 0.04. Ctrl, control; Densi, densitometric; d, days.

sensitivity in oASC-derived adipocytes, we cultured oASC-derived adipocytes for 24 h in conditioned medium obtained at different intervals from cASC-derived adipocytes (cCM). None of the cCM samples tested increased insulin-induced glucose uptake by oASC-derived adipocytes (Fig. 3D) nor resulted in phosphorylation of IRS1 protein (Fig. 3F). However, in the reverse experiment, insulin sensitivity and IRS1 phosphorylation were both impaired in cASC-derived adipocytes upon culture in conditioned medium from 7-day differentiated oASC-derived adipocytes (oCM; Fig. 3E and F). No changes were observed in the differentiation capacity of cASC after oCM treatment or on the gene expression profile, except from a significant decrease in IRS2 expression (Supplementary Fig. 2A and B). Thus, factors secreted by oASC-derived adipocytes are able to induce insulin resistance in cASC-derived adipocytes, but conditioned medium from control cells is unable to restore the control phenotype on obese cells.

To further analyze the results obtained with the oCM and to determine if the highly expressed cytokines TNF-α or MCP-1 in oASC were the cause of their phenotype, we performed firstly a 7-day differentiation protocol of cASC in the presence of these cytokines and also a separate protocol of differentiation of oASC in the presence of specific inhibitory antibodies against TNF-α or MCP-1. Interestingly, the accumulation of lipids was not affected by these treatments in ASCs, indicating that the hyperplasic phenotype observed previously with oASC-derived adipocytes was independent of these factors (Fig. 3G). Nevertheless, when we repeated these treatments on 7-day cASC-derived adipocytes or on oASC-derived adipocytes and measured glucose uptake, we observed that the presence of TNF-α provoked insulin-resistance on cASCs, whereas the treatment with inhibitory antibodies against TNF-α induced insulin-sensitivity on oASCs (Fig. 3H). In fact, when glucose uptake was measured in cASCs

treated with oCM together with antibodies against TNF-α, the insulin nonresponding phenotype disappeared (Supplementary Fig. 2C). Furthermore, IRS2 expression, but not aP2, was consistently modified by controlling the activity of the TNF-α cytokine (Fig. 3I). In contrast, modification of MCP-1 activity seemed not to have any effect on glucose uptake or IRS2 expression (Fig. 3H and I). Therefore, these results point to TNF-α as a factor that could be mediating the insulin-resistance phenotype on oASCs.

Cytosol transfer from cASCs rescues metabolic responsiveness in oASCs. Given that the conditioned medium from cASCs was unable to improve the insulin sensitivity in obese-derived cells and that the high levels of TNF-α found in oASCs could only block their response to insulin but did not affect their differentiation ability or lipid accumulation, we hypothesized that the phenotype of mature oASC-derived adipocytes could be determined by activation of internal signaling pathways, as shown recently for other adult reprogramming protocols (26,27). We tested this possibility by using a new approach in which cellular fractions isolated from cASCs are transferred to oASCs before exposure to the differentiation stimulus. Nuclear fractions (NFs) and CFs of cASCs were prepared using a commercial cell fractionation kit (Fig. 4A). To serve as controls, subcellular fractions were also obtained from murine fibroblasts and from oASCs (Supplementary Fig. 3). Each fraction was assessed by agarose gel electrophoresis and by Western blot for products that define each compartment. Thus, DNA was detected only in the NF, and the CF was positive for glyceraldehyde-3-phosphate dehydrogenase (GADPH) protein, while the NF was positive for SP1 (nucleic acid binding protein; Fig. 4B). These fractions were delivered into oASCs using the ProdeliverIN lipid-based protein-capture reagent. Delivery of NF caused some cell death, because a proportion of cells lost adherence to the plate, but most remaining
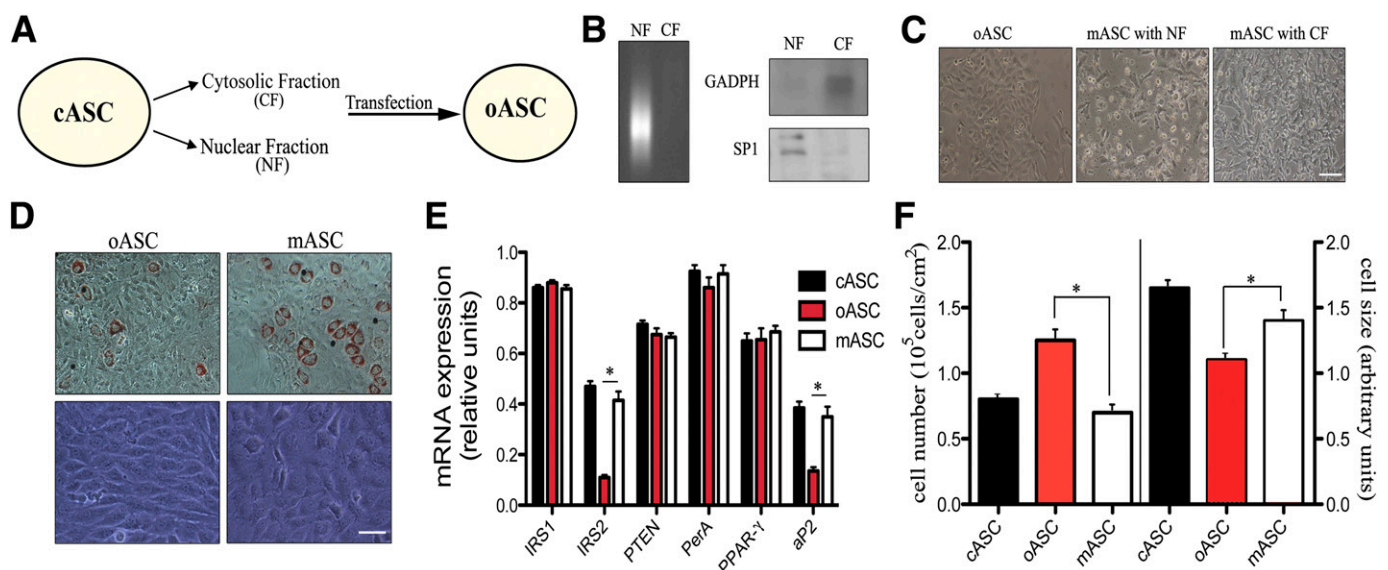
FIG. 4. Isolation and delivery of ASC subcellular fractions. *A:* Scheme for the isolation of cASC subcellular fractions and their transfer into oASCs. *B:* NFs and CFs were analyzed by agarose gel electrophoresis and Western blot for GADPH (cytosol marker) and SP1 (nuclear marker). A representative of three experiments is shown. *C:* Representative images of oASCs after transfer of NF or CF, called mASC, are shown (*n* = 8). Bar, 50 μm. *D:* Light microscopy and Oil Red O staining in adipocyte cultures differentiated (7 days) from oASCs and mASCs (CF transferred). Representative images are shown (*n* = 8). Bar, 30 μm. *E:* Gene expression profile after delivering of mASC (*n* = 5). *P < 0.02. *F:* Cell number (*left*) and cell size (*right*) analyzed by flow cytometry in oASCs and mASCs (*n* = 5).

cells continued to proliferate (Fig. 4C). In contrast, CF appeared to have no effect on oASC viability or proliferation (Fig. 4C). Because no toxic effects were detected with CF, this fraction was selected for subsequent evaluation. After delivery of CF, the modified oASCs (termed mASC) were cultured in differentiation medium, and their progress toward mature adipocytes was monitored as before. Compared with oASCs, mASC-derived adipocytes recovered the normal morphology of cASC-derived adipocytes and formed defined mature adipocytes, with lipid accumulation evident after 5 days of differentiation (Fig. 4D). No effect could be observed in oASC transferred with CF derived from fibroblasts (fCF) or in cASCs transferred with the CF derived from oASC (oCF) (Supplementary Fig. 3A). The establishment of a mature adipocyte morphology in mASCs was accompanied by an increase of IRS2 and aP2 expression levels compared with oASCs (Fig. 4E) and a decrease in cell number together with an increased cell size (Fig. 4F). Again, no major changes were observed in the expression level of IRS2 or aP2 in oASC transferred with fCF or in cASC transferred with oCF (Supplementary Fig. 3B). Taken together, these results suggested a restoration of a mature phenotype in oASCs when transfected with a CF of cASCs.

To assess the physiological significance of this restoration, we next measured glucose uptake as an indicator of functionality in ASCs. Interestingly, adipocytes derived from mASCs, but not oASCs, had a low basal glucose uptake and exhibited insulin sensitivity similar to that of cASCs (Fig. 5A). No major differences were detected on oASCs transferred with fCF or in cASCs transferred with oCF (Supplementary Fig. 3C). Moreover, mASC-derived adipocytes recovered cASC-like insulin responses with regards to GLUT4 transportation (Fig. 5B) and IRS1 phosphorylation (Fig. 5C). Finally, examination of the secretion profile of mASC-derived adipocytes showed that delivery of CF significantly increased adiponectin release and decreased the release of MCP-1 and TNF-α compared with oASCs (Fig. 5D). Also, mASCs presented a similar ability to differentiate into other tissues (Supplementary Fig. 3D). None of the above effects was observed when fCF was used to transfect oASCs, suggesting specifically that a component, or components of ASCs was necessary to reprogram oASCs. In conclusion, delivery of a CF derived from cASCs is able to restore insulin sensitivity and the capacity for adipocyte maturation in oASCs.

Lin28 blocks *Let7* microRNA expression and restores glucose metabolism in oASCs. To investigate the potential mechanism(s) for this reprogramming process, we examined the CF of cASCs in more detail. Cytosolic fractions were treated with proteinase-k to inactivate the protein compartment or with an RNAse/DNAse cocktail to degrade nucleic acids, before transfection. As shown in Fig. 6A, oASCs transfected with a protein-inactivated fraction, followed by differentiation (CFp-mASCs), failed to recover glucose uptake compared with recovered oASCs transfected with a nonmodified CF (CF-mASCs; Fig. 6A). Moreover, cell size and cell number of CFp-mASCs were both significantly different from control cells (CF-mASCs; Fig. 6B). In contrast, when DNA and RNA was degraded in the CF with an RNAse/DNAse cocktail, before transfection into oASCs, the resulting modified cells (CFr-mASCs) were equivalent to CF-mASC control cells in glucose uptake (Fig. 6A) and cell size (Fig. 6B), suggesting that a cytosolic protein component was likely responsible for this reprogramming phenomenon.
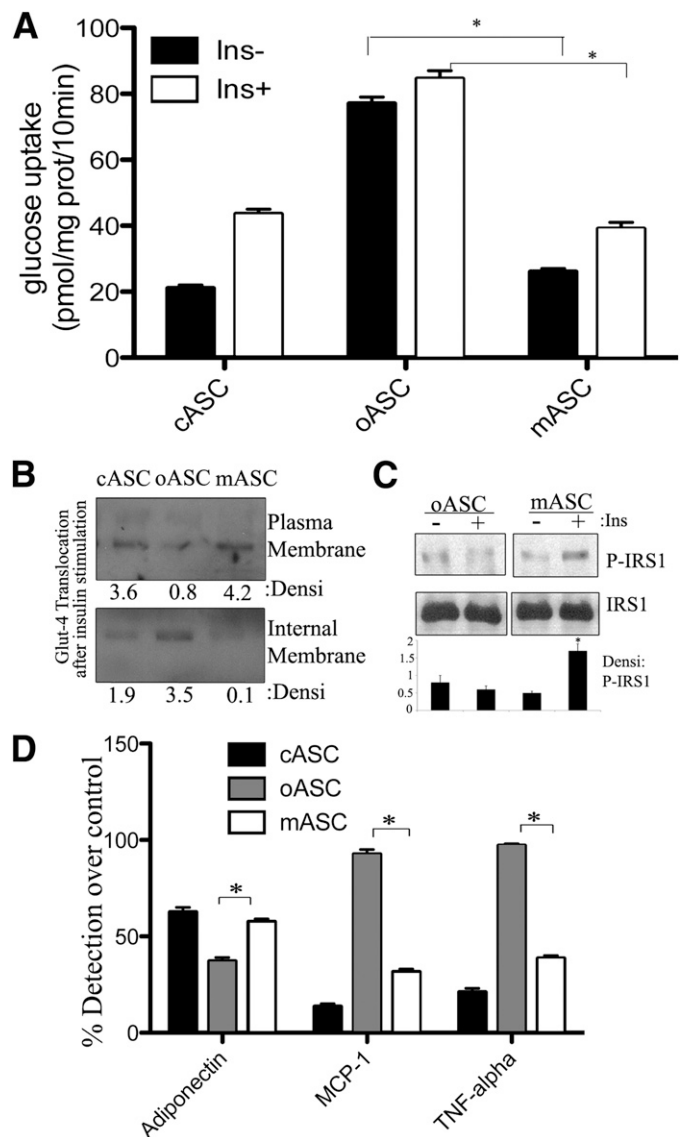
FIG. 5. Transfer of cASC cytosol to oASCs restores nonobese metabolic parameters. *A*: Insulin-stimulated glucose uptake by adipocytes differentiated (7 days) from cASCs, oASCs, and mASCs. Adipocyte cultures were maintained overnight in serum-free, low-glucose medium and then stimulated with 10 nmol/L insulin (30 min; *n* = 6). *$*P < 0.01$ between mASCs and oASCs. *B* and *C*: GLUT4 expression and IRS phosphorylation are restored in 7-day differentiated mASCs. cASCs, oASCs, and mASCs were stimulated with 10 nmol/L insulin for 10 min, and membrane fractions or cell lysates were probed by Western blot with anti–GLUT4 or anti-IRS1 antibodies. Densitometric quantification of three independent membranes is shown. *$*P < 0.03$. *D*: Adiponectin, MCP-1, and TNF-α production by oASCs and mASCs. Cells were cultured overnight in serum-free medium, and adiponectin, MCP-1, and TNF-α were detected by immunoassay. Results are expressed as the percentage of detection comparing undifferentiated ASC at day 0 to differentiated ASC at day 7 (*n* = 6). *$*P < 0.02$ between mASCs and oASCs. Densi, densitometric; Ins, insulin; prot, protein.

Zhu et al. (28) recently described an important contribution of the Lin28/*Let7* microRNA pathway to glucose metabolism in mice, and interestingly, this pathway has also been implicated in the propensity for differentiation in embryonic stem cells (28,29). Given that these two disparate processes were altered in our ASC samples, we wondered whether the Lin28/*Let7* axis might be playing a role in ASC differentiation and/or maturation. Thus CFs of various ASCs were analyzed for the presence of the
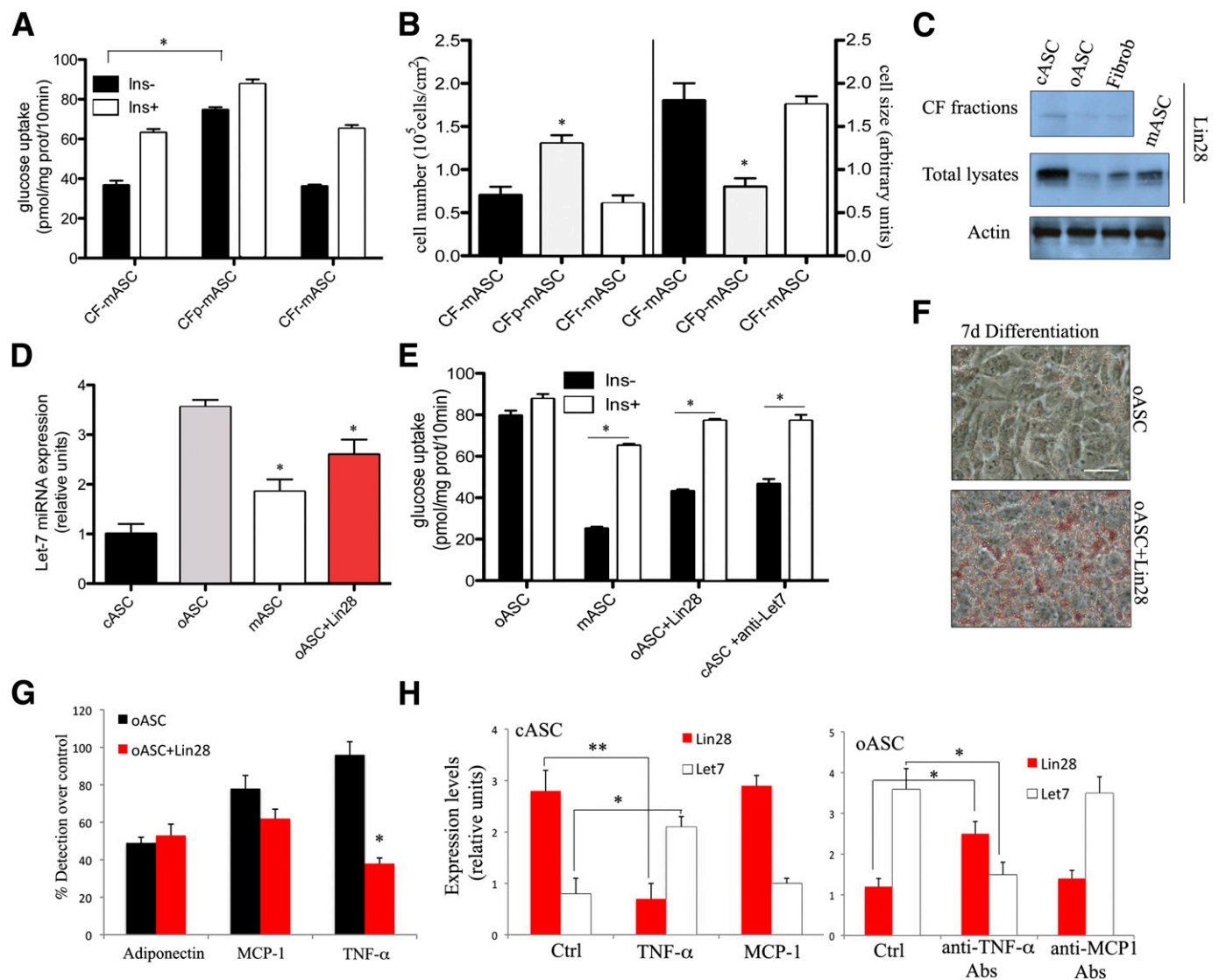
FIG. 6. Analysis of the CF content and its action mechanism. *A* and *B*: CFs, inactivated by proteinase-k (CFp) or by RNase cocktail (CFr), were delivered into oASC. Glucose uptake and the cell size-to-cell number ratio were measured in mASCs (*n* = 5). *P < 0.05. *C*: Analysis of Lin28 protein expression by Western blot in oASC-derived or cASC-derived CFs or in whole ASC lysates to note the restoration of Lin28 levels after cASC-derived CF (cCF) delivery into oASC (mASC). One representative image of three independent experiments is shown. *D*: *Let7* microRNA expression was analyzed by RT-PCR (*n* = 5). *P < 0.04. *E*: Insulin-stimulated glucose uptake by adipocytes differentiated (7 days) from modified oASCs or oASC delivered with Lin28 protein. Adipocyte cultures were maintained overnight in serum-free, low-glucose medium and then stimulated with 10 nmol/L insulin (30 min; *n* = 5). *P < 0.03 between oASCs and mASCs or oASCs+Lin28. *F*: Representative images of Oil Red O–stained oASCs and oASC delivered with Lin28 protein after 7 days of differentiation into mature adipocytes (*n* = 5). Bar, 30 μm. *G*: Adiponectin, MCP-1, and TNF-α production by oASC-derived adipocytes (7 days) transferred or not with Lin28 and detected by immunoassay. Results are expressed as the percentage of detection comparing undifferentiated oASCs at day 0 to differentiated oASCs at day 7 (*n* = 5). *P < 0.02. *H*: *Let7* microRNA and Lin28 expression were analyzed by RT-PCR in cASC-derived adipocytes (7 days) in the presence or absence of 1 ng/mL TNF-α or 0.2 ng/mL MCP-1 cytokines and in oASC-derived adipocytes in the presence or absence of 10 ng/mL anti–TNF-α or anti–MCP-1 antibodies (Abs) (*n* = 5). *P < 0.05 and **P < 0.02. d, days; Fibrob, fibroblast.

microRNA binding protein Lin28 protein by Western blotting. As shown in Fig. 6*C*, although Lin28 protein could be detected in total lysates from all cells tested, the absolute quantity of Lin28 was significantly higher in total lysates and CF of cASCs compared with oASC cells and also fibroblasts. To confirm that the proteins transferred with this method and, specifically Lin28, remained stable, metabolic labeling of cASC was performed; labeled proteins and immunoprecipitation of labeled Lin28 were recovered from whole lysates and CFs of cASC or mASC (Supplementary Fig, 3*E*). Furthermore, after transfection of cASC-derived CF into oASCs, the levels of Lin28 protein were restored in the obese-derived ASCs, as

determined by Western blotting (mASC; Fig. 6*C*). As anticipated, expression of *Let7* miRNA, a major binding partner of Lin28, was reciprocally regulated in ASC populations compared with Lin28, with higher expression observed in oASCs and significantly less expression found in cASCs (Fig. 6*D*). In addition, transfection of cASC-derived CF to oASCs caused a decrease in the expression of *Let7* (Fig. 6*D*). Indeed, using the identical lipid-based protein transfer protocol, delivery of purified Lin28 protein into oASCs largely mirrored the effects of cASC-derived CF delivery with respect to decreasing the expression of *Let7* (Fig. 6*D*). Intriguingly, together with modifying the expression of *Let7* transfection of Lin28

protein alone could also restore insulin sensitivity (Fig. 6*E*) to oASCs as well as provoke a mature phenotype (Fig. 6*F*).

Finally, to confirm that the results observed were partly due to the reduction of *Let7* expression, we used a parallel strategy by directly inhibiting *Let7* expression using a LNA-based *Let7* inhibitor (Exiqon). As shown in Fig. 6*E*, the inhibition of *Let7* microRNA significantly restored insulin sensitivity to oASC. Thus, our results show that CF delivery of Lin28 can repress *Let7* activity and therefore restore insulin pathways and adipocyte differentiation. To analyze the existence of a communication between this Lin28 pathway and the TNF-α pathway, we measured the quantity of TNF-α secreted after Lin28 transfection of oASC. Interestingly, levels of TNF-α, but not MCP1, were partially reduced (Fig. 6*G*). In fact, the communication was bidirectional, because the treatment of cASC with TNF-α modified the expression levels of Lin28 and *Let7*, and also, the treatment of oASC with inhibitory antibodies against TNF-α changed the levels of both molecules (Fig. 6*H*). These experiments indicate that the inflammatory cytokine TNF-α activates a circuit that involves Lin28/*Let7* axis, provoking insulin resistance and hyperplasic phenotype.

Metabolic properties of hASCs. Having established the importance of the environmental origin for determining the differentiation properties of mouse ASCs, we wondered if hASCs are similarly regulated. We therefore examined cell morphology, insulin sensitivity, and lipid accumulation in hASCs from five nonobese (chASCs) patients (BMI 22 kg/m^2) and five obese (ohASCs) patients (BMI 31 kg/m^2) in parallel to one commercial sample of hASCs of each type. After confirming the phenotype of the isolated hASCs (Supplementary Fig. 4*A–C*) we found that, consistent with our results from mouse cells and previous work by others (30,31), hyperplasia, together with a reduced cell size and impaired maturation, were observed in ohASC cultures at day 14 of culture (Fig. 7*A*). After differentiation for 14 days, chASCs exhibited insulin-sensitivity by increasing their glucose uptake after insulin stimulation (Fig. 7*B*). In contrast, parallel cultures of ohASCs, although exhibiting a higher basal level of glucose uptake, were nonresponsive to insulin (Fig. 7*B*). Similarly, ohASCs exhibited a reduced glycerol release after adrenergic stimulation compared with chASCs, which again were non-responsive to insulin (Fig. 7*C*). Analogous to the results observed in mouse cells, differentiated ohASCs showed increased secretion of MCP-1 and TNF-α and a reduction of adiponectin levels (Fig. 7*D*). Collectively, these results suggest that human obese cells behave similarly to the equivalent mouse populations in their failure to respond properly to metabolic stimulation.

Finally, to determine whether delivery of subcellular fractions could restore normal metabolism in ohASCs, we isolated CF and NFs from chASCs, as before. Once again, CF was selected for delivery due to its nontoxicity (data not shown). Delivery of CF to ohASCs before differentiation increased their glucose uptake and the capacity for glycerol release (Fig. 7*B* and *C*). Moreover, these modified ohASCs (mhASC) recovered the cytokine profile of chASCs and their ability for full differentiation into mature adipocytes (Fig. 7*D* and *E*). CF was analyzed for the presence of Lin28 protein, and as shown in Fig. 7*F*, chASC-derived CF was enriched in this protein compared with ohASC-derived CF, as well as total lysates derived from cASC or mASC (CF-delivered oASC) were enriched similarly. As anticipated, *Let7* microRNA expression was reduced in lysates derived from ohASCs previously delivered with mhASC or with purified Lin28 protein compared with nontreated ohASCs and reached similar levels to chASCs (Fig. 7*G*). Finally, mhASCs, Lin28-delivered, or anti–*Let7*-treated ohASCs overcame the limited differentiation of ohASCs and recovered insulin sensitivity (Fig. 7*E* and *H*).

DISCUSSION

The findings presented here demonstrate that the potential of ASCs for correct functional activity and terminal differentiation depends on the environment from where they are isolated. ASCs derived from a nonobese environment expressed most of the genes related to mature adipocytes, except for IRS2, implicated in insulin signaling, and aP2, implicated in lipids droplets formation. cASC-derived adipocytes were insulin-sensitive, whereas oASCs-derived adipocytes were insulin resistant and presented a hyperplasic phenotype. The obese environment impairs GLUT4 translocation to the plasma membrane and insulin signaling via IRS and thus limits the ability of oASCs to generate correct, well-functioning adipocytes. This in vitro finding likely reflects the chronic elevation of insulin during insulin-resistant states observed in overweight individuals (32,33) and indicates that although ASCs can be present in obese patients, their contribution to adipose tissue homeostasis will be impaired and their effect detrimental rather than beneficial. In contrast, in healthy adipose tissue, ASCs would contribute to tissue homeostasis by generating new, properly functioning adipocytes.

An alteration in the lipolytic pathway is thought to be one of the main mechanisms linking insulin resistance to hyperlipidemia in obesity and type 2 diabetes (34). In our studies and in contrast to cASCs, oASCs exhibit an increase in their basal lipolytic rate, a decrease in iso-proterenol responsiveness, and an impaired inhibition of lipolysis by insulin. Interestingly, oASCs also present a deficiency in the internal accumulation of lipids and tri-glycerides, which could account for the excessive lipid accumulation in nonadipose tissues (lipotoxicity) observed in obese patients (35,36).

Another finding from this study was that the environmental origin influenced the secretion profile of ASCs and derived adipocytes. Thus, whereas differentiation of cASCs was associated with increased adiponectin secretion, this was impaired in differentiating oASCs, in agreement with the inverse correlation of adiponectin with insulin-resistance (37). In contrast, secretion of proin-flammatory cytokines and release of NEFA were markedly stimulated in oASCs differentiated for 7 days. Indeed, elevated plasma concentrations of MCP-1, TNF-α, and NEFA have been detected in obese and diabetic patients (38–40). The decrease in adiponectin expression with differentiation of oASCs contrasts with the progressive increase in differentiating cASCs. Downregulation of adiponectin expression during prolonged culturing might be a consequence of increased NEFA release, as previously described in murine adipocytes (41).

The high levels of TNF-α found in differentiated oASCs seem to interfere with the ability of oASCs to respond to insulin but do not directly affect their differentiation ability. Although TNF-α has been implicated in the regulation of lipolysis and differentiation of adipocytes (32,42), in our ASC population, this molecule appeared to regulate only glucose uptake and not lipogenesis or differentiation
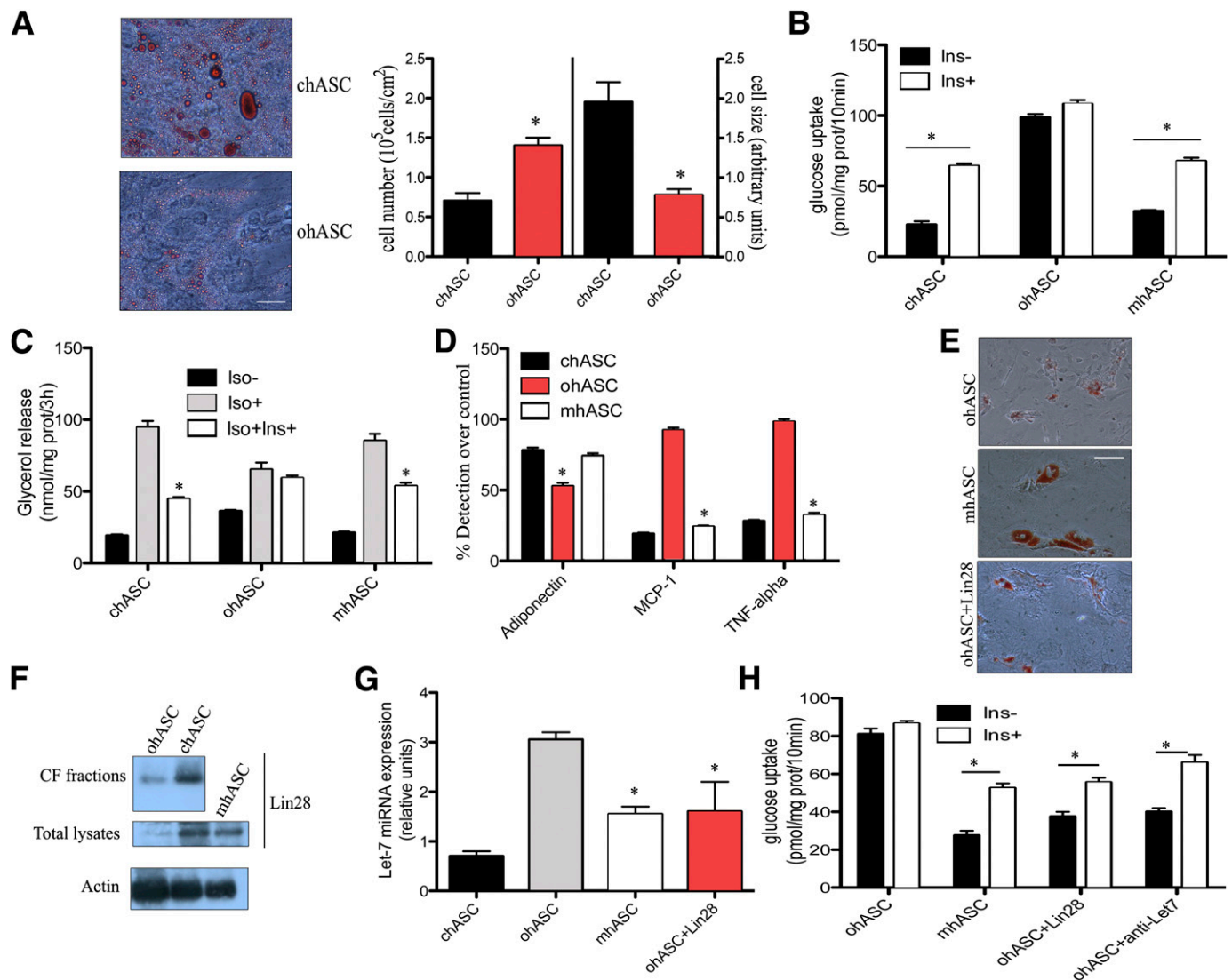
FIG. 7. hASCs show similar obesity-related differentiation and metabolic alterations, which are rescued by transfer of cytosol from chASCs. *A*: Representative image of Oil Red O staining in chASC and ohASC differentiated for 14 days into adipocytes (*n* = 5 + 1). Bar, 30 μm. Cell number (*left*) and cell size (*right*) analyzed by flow cytometry in chASCs and ohASCs at day 14 of differentiation (*n* = 6). *P < 0.04. *B*: Insulin-stimulated glucose uptake by cASCs, oASCs, and cytosol-modified hASCs at 14-day differentiation. Cultures were stimulated with 10 nmol/L insulin (Ins) for 30 min, and results are expressed as pmol/mg of prot (prot)/10 min (*n* = 6). *P < 0.03. *C*: Glycerol release by cASCs, oASCs, and modified hASCs after 14-day differentiation. Cells were stimulated with 10 nmol/L Ins for 1 h before stimulation with 1 μmol/L isoproterenol (Iso) for 15 min. Results are expressed as nmol/mg of protein/3 h (*n* = 6). *P < 0.04. *D*: Adiponectin, MCP-1, and TNF-α production by hASCs. cASCs, oASCs, and modified hASCs were cultured overnight in serum-free medium, and adiponectin, MCP-1, and TNF-α were detected by immunoassay. Results are expressed as the percentage of detection comparing undifferentiated hASC at day 0 to differentiated hASC at day 14 (*n* = 6). *P < 0.03. *E*: Representative images of Oil Red O stained mhASC, ohASCs, and ohASC delivered with Lin28 protein after 14-day differentiation into mature adipocytes (*n* = 6). Bar, 30 μm. *F*: Analysis of Lin28 protein expression in ohASC-derived or cASC-derived CFs or in whole ASC lysates by Western blot. One of five independent experiments is shown. *G*: *Let7* microRNA expression was analyzed by RT-PCR (*n* = 6). *P < 0.05. *H*: Insulin-stimulated glucose uptake by adipocytes differentiated (14 days) from obese modified hASCs, ohASC delivered with Lin28 protein or treated with anti-Let 7 inhibitor. Adipocyte cultures were maintained overnight in serum-free, low-glucose medium and then stimulated with 10 nmol/L insulin (30 min; *n* = 6). *P < 0.02.

measured by red oil accumulation. Indeed, the inability of conditioned medium from cASCs to restore insulin sensitivity in oASC-derived adipocytes or the treatment with inhibitory antibodies against TNF-α to restore the hyperplasic phenotype suggest that the phenotype of mature oASC-derived adipocytes is determined by activation of internal signaling pathways. We tested this possibility by using a new approach in which CFs isolated from cASCs are transferred to oASCs before exposure to the differentiation stimulus. Delivery of subcellular fractions has been previously demonstrated to induce phenotypic changes in recipient cells (27). In our study, cASC CFs restored

insulin-stimulated glucose uptake in oASC-derived adipocytes and restored insulin-induced IRS phosphorylation. Moreover, using this approach, we have demonstrated that the Lin28/*Let7* axis is implicated in the regulation of ASC differentiation and insulin metabolism. Lin28 protein appeared in the cytosol CF and restored an insulin-sensitized state in the oASCs. We believe that microRNA *Let7* may be inhibiting known target genes in the oASCs such as Irs2, Insr, and Igf1r, whereas Lin28 protein could be controlling the PI3k/AKT pathways, as previously described for both components (28). This situation will generate an insulin-resistant state in oASC. In fact, Lin28 has been

implicated in the repression of microRNA *Let7* and mediates both glucose metabolism and embryonic stem cell differentiation (28,29,43). Interestingly, the existence of a feedback loop involving nuclear factor-κB, Lin28/*Let7* and TNF-α has been described in transformed cells that maintains the transformed state (44). This regulatory circuit could link inflammation to the cellular insulin-resistant state. Finally, our data clearly indicate that the basic metabolic mechanisms are similar in mouse and human ASCs, and that ASCs from obese human patients are equally susceptible to enhancement by transfer of cytosol from healthy ASCs.

Current treatments for the restoration of insulin sensitivity are based on pharmacological intervention and have revealed different unwanted side effects (32,45,46). The cytosol transfer technique offers the possibility of correcting the phenotype of ASCs isolated from obese patients in vitro, and in the future, we postulate that this tool could be used in vivo to generate new proper-functioning adipocytes.

REFERENCES

1. San Martín N, Gálvez BG. A new paradigm for the understanding of obesity: the role of stem cells. Arch Physiol Biochem 2011;117:188–194
2. Zeve D, Tang W, Graff J. Fighting fat with fat: the expanding field of adipose stem cells. Cell Stem Cell 2009;5:472–481
3. Rodeheffer MS, Birsoy K, Friedman JM. Identification of white adipocyte progenitor cells in vivo. Cell 2008;135:240–249
4. Majka SM, Barak Y, Klemm DJ. Concise review: adipocyte origins: weighing the possibilities. Stem Cells 2011;29:1034–1040
5. Awad H, Halvorsen YDC, Gimble JM, Guilak F. Effects of TGF-beta1 and dexamethasone on growth and chondrogenic differentiation of adipose derived stromal cells in vitro. Tissue Eng 2003;9:1301–1312
6. Gimble JM, Guilak F. Differentiation potential of adipose derived adult stem (ADAS) cells. Curr Top Dev Biol 2003;58:137–160
7. Mizuno H, Zuk PA, Zhu M, Lorenz HP, Benhaim P, Hedrick MH. Myogenic differentiation by human processed lipoaspirate cells. Plast Reconstr Surg 2002;109:199–209; discussion 210–211
8. Zuk PA, Zhu M, Mizuno H, et al. Multilineage cells from human adipose tissue: implications for cell-based therapies. Tissue Eng 2001;7:211–228
9. Locke M, Feisst V, Dunbar PR. Concise review: human adipose-derived stem cells: separating promise from clinical need. Stem Cells 2011;29:404–411
10. Cao Y. Angiogenesis modulates adipogenesis and obesity. J Clin Invest 2007;117:2362–2368
11. Brunner EJ, Kivimäki M, Witte DR, et al. Inflammation, insulin resistance, and diabetes—Mendelian randomization using CRP haplotypes points upstream. PLoS Med 2008;5:e155
12. MacDougald OA, Mandrup S. Adipogenesis: forces that tip the scales. Trends Endocrinol Metab 2002;13:5–11
13. Spalding KL, Arner E, Westermark PO, et al. Dynamics of fat cell turnover in humans. Nature 2008;453:783–787
14. Spiegelman BM, Flier JS. Obesity and the regulation of energy balance. Cell 2001;104:531–543
15. Danforth E Jr. Failure of adipocyte differentiation causes type II diabetes mellitus? Nat Genet 2000;26:13
16. Weber RV, Buckley MC, Fried SK, Kral JG. Subcutaneous lipectomy causes a metabolic syndrome in hamsters. Am J Physiol Regul Integr Comp Physiol 2000;279:R936–R943
17. Cederberg A, Enerbäck S. Insulin resistance and type 2 diabetes—an adipocentric view. Curr Mol Med 2003;3:107–125
18. Clément K, Vaisse C, Lahlou N, et al. A mutation in the human leptin receptor gene causes obesity and pituitary dysfunction. Nature 1998;392:398–401
19. Gálvez BG, San Martín N, Rodríguez C. TNF-alpha is required for the attraction of mesenchymal precursors to white adipose tissue in Ob/ob mice. PLoS ONE 2009;4:e4444
20. Bunnell BA, Flaat M, Gagliardi C, Patel B, Ripoll C. Adipose-derived stem cells: isolation, expansion and differentiation. Methods 2008;45:115–120
21. San Martin N, Cervera AM, Cordova C, Covarello D, McCreath KJ, Galvez BG. Mitochondria determine the differentiation potential of cardiac meso-angioblasts. Stem Cells 2011;29:1064–1074
22. de Alvaro C, Teruel T, Hernandez R, Lorenzo M. Tumor necrosis factor alpha produces insulin resistance in skeletal muscle by activation of inhibitor kappaB kinase in a p38 MAPK-dependent manner. J Biol Chem 2004;279:17070–17078
23. Minasi MG, Riminucci M, De Angelis L, et al. The meso-angioblast: a multipotent, self-renewing cell that originates from the dorsal aorta and differentiates into most mesodermal tissues. Development 2002;129:2773–2783
24. Ahima RS. Adipose tissue as an endocrine organ. Obesity (Silver Spring) 2006;14(Suppl. 5):242S–249S
25. Ouchi N, Parker JL, Lugus JJ, Walsh K. Adipokines in inflammation and metabolic disease. Nat Rev Immunol 2011;11:85–97
26. Song K, Nam YJ, Luo X, et al. Heart repair by reprogramming non-myocytes with cardiac transcription factors. Nature 2012;485:599–604
27. Kim TK, Sul JY, Peternko NB, et al. Transcriptome transfer provides a model for understanding the phenotype of cardiomyocytes. Proc Natl Acad Sci USA 2011;108:11918–11923
28. Zhu H, Shyh-Chang N, Segrè AV, et al.; DIAGRAM Consortium; MAGIC Investigators. The Lin28/let-7 axis regulates glucose metabolism. Cell 2011;147:81–94
29. Martinez NJ, Gregory RI. MicroRNA gene regulatory pathways in the establishment and maintenance of ESC identity. Cell Stem Cell 2010;7:31–35
30. Oñate B, Vilahur G, Ferrer-Lorente R, et al. The subcutaneous adipose tissue reservoir of functionally active stem cells is reduced in obese patients. FASEB J 2012;26:4327–4336
31. Roldan M, Macias-Gonzalez M, Garcia R, Tinahones FJ, Martin M. Obesity short-circuits stemness gene network in human adipose multipotent stem cells. FASEB J 2011;25:4111–4126
32. Fernández-Veledo S, Nieto-Vazquez I, de Castro J, et al. Hyperinsulinemia induces insulin resistance on glucose and lipid metabolism in a human adipocytic cell line: paracrine interaction with myocytes. J Clin Endocrinol Metab 2008;93:2866–2876
33. Weyer C, Hanson RL, Tataranni PA, Bogardus C, Pratley RE. A high fasting plasma insulin concentration predicts type 2 diabetes independent of insulin resistance: evidence for a pathogenic role of relative hyperinsulinemia. Diabetes 2000;49:2094–2101
34. Bergman RN, Mittelman SD. Central role of the adipocyte in insulin resistance. J Basic Clin Physiol Pharmacol 1998;9:205–221
35. Unger RH, Zhou YT. Lipotoxicity of beta-cells in obesity and in other causes of fatty acid spillover. Diabetes 2001;50(Suppl. 1):S118–S121
36. Schaffer JE. Lipotoxicity: when tissues overeat. Curr Opin Lipidol 2003;14:281–287

37. Hotta K, Funahashi T, Bodkin NL, et al. Circulating concentrations of the adipocyte protein adiponectin are decreased in parallel with reduced insulin sensitivity during the progression to type 2 diabetes in rhesus monkeys. Diabetes 2001;50:1126–1133

38. Takahashi K, Mizuarai S, Araki H, et al. Adiposity elevates plasma MCP-1 levels leading to the increased CD11b-positive monocytes in mice. J Biol Chem 2003;278:46654–46660

39. Kern PA, Ranganathan S, Li C, Wood L, Ranganathan G. Adipose tissue tumor necrosis factor and interleukin-6 expression in human obesity and insulin resistance. Am J Physiol Endocrinol Metab 2001;280:E745–E751

40. Roden M. How free fatty acids inhibit glucose utilization in human skeletal muscle. News Physiol Sci 2004;19:92–96

41. Shintani M, Nishimura H, Yonemitsu S, et al. Downregulation of leptin by free fatty acids in rat adipocytes: effects of triacsin C, palmitate, and 2-bromopalmitate. Metabolism 2000;49:326–330

42. Fernández-Veledo S, Vila-Bedmar R, Nieto-Vazquez I, Lorenzo M. c-Jun N-terminal kinase 1/2 activation by tumor necrosis factor-alpha induces insulin resistance in human visceral but not subcutaneous adipocytes: reversal by liver X receptor agonists. J Clin Endocrinol Metab 2009;94:3583–3593

43. Piskounova E, Polytarchou C, Thornton JE, et al. Lin28A and Lin28B inhibit let-7 microRNA biogenesis by distinct mechanisms. Cell 2011;147:1066–1079

44. Iliopoulos D, Hirsch HA, Struhl K. An epigenetic switch involving NF-kappaB, Lin28, Let-7 MicroRNA, and IL6 links inflammation to cell transformation. Cell 2009;139:693–706

45. Kopelman PG. Obesity as a medical problem. Nature 2000;404:635–643

46. Lughetti L, China M, Berri R, Predieri B. Pharmacological treatment of obesity in children and adolescents: present and future. J Obes 2011;2011:928165